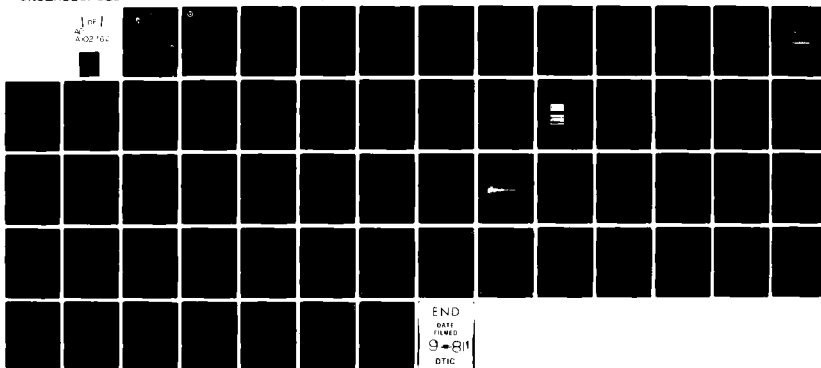


AD-A102 762 JOHNS HOPKINS UNIV BALTIMORE MD DEPT OF MATERIALS SC--ETC F/8 20/11
ACOUSTIC EMISSION DETERMINATION OF DEFORMATION MECHANISMS LEADIN--ETC(U)
JUL 81 J T GLASS, S MAJEROWICZ, R E GREEN N00024-80-C-5337
DTNSRDC/SME-81-44 NL

UNCLASSIFIED

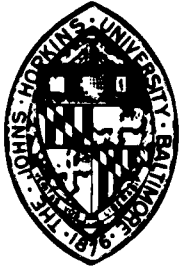


END
FILE NUMBER
9-811
DTIC

18 DTNSRDC Report SME 81-44 19
AD A102762

LEVEL

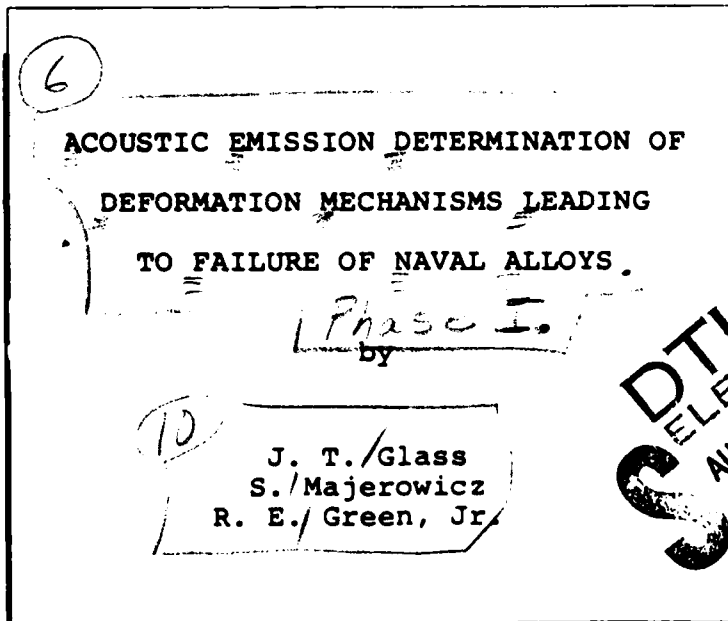
12



THE JOHNS HOPKINS UNIVERSITY

MATERIALS SCIENCE AND ENGINEERING
DEPARTMENT

DTIC FILE COPY



9 Rep. for Jan 1981
Prepared for
Naval Sea Systems Command (SEA 05R15)
and
David Taylor Naval Ship R&D Center (Code 28)
under
Contract N00024-80-C-5337

15 Jul 81

12 60

APPROVED FOR PUBLIC RELEASE; DISTRIBUTION UNLIMITED

81 8 12 005 411993



DEPARTMENT OF THE NAVY
DAVID W. TAYLOR NAVAL SHIP RESEARCH
AND DEVELOPMENT CENTER
HEADQUARTERS
BETHESDA, MARYLAND 20904

ANNAPOLIS LABORATORY
ANNAPOLIS, MD 21402
CARDEROCK LABORATORY
BETHESDA, MD 20904

IN REPLY REFER TO:

2820:CAZ
3900
DTNSRDC/SME 81-44

10 AUG 1981

From: Commander, David Taylor Naval Ship R&D Center
To: Distribution List

Subj: Acoustic Emission Exploratory Development

Ref: (a) Submarine Materials Block Program, SF6154/591, Task 20456

Encl: (1) The Johns Hopkins University, Materials Science and Engineering Department Report (SME 81-44), "Acoustic Emission Determination of Deformation Mechanisms Leading to Failure of Naval Alloys", prepared under Contract N00024-80-C-5337.

1. As part of reference (a) the David Taylor Naval Ship Research and Development Center (DTNSRDC) is monitoring a three phase program being conducted to determine deformation mechanisms in Naval alloys, using acoustic emission signals detected by optical techniques. Enclosure (1) is forwarded herewith and presents the results of phase I of the program.

J. R. GRISCI
By direction

Copy to:

Distribution of enclosure (1)

UNCLASSIFIED

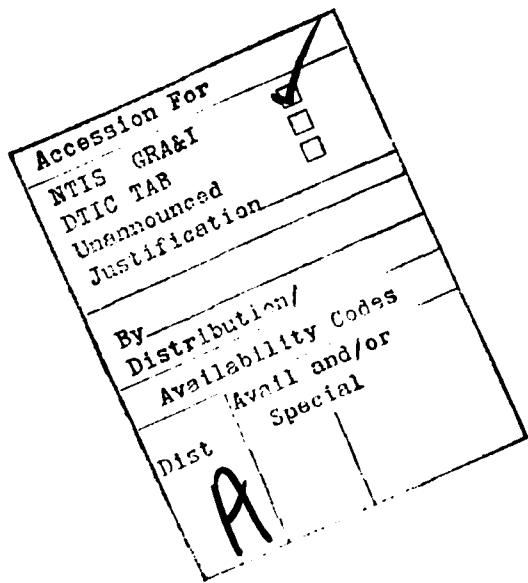
SECURITY CLASSIFICATION OF THIS PAGE (When Data Entered)

REPORT DOCUMENTATION PAGE		READ INSTRUCTIONS BEFORE COMPLETING FORM
1. REPORT NUMBER DTNSRDC/SME 81-44	2. GOVT ACCESSION NO. AD-A102 762	3. RECIPIENT'S CATALOG NUMBER
4. TITLE (and Subtitle) Acoustic Emission Determination of Deformation Mechanisms Leading to Failure of Naval Alloys	5. TYPE OF REPORT & PERIOD COVERED Phase I January 1980-December 1980	
7. AUTHOR(s) J. T. Glass, S. Majerowicz, R. E. Green, Jr.	8. CONTRACT OR GRANT NUMBER(s) N00024-80-c-5337	
9. PERFORMING ORGANIZATION NAME AND ADDRESS The Johns Hopkins University Materials Science & Engineering Dept. Baltimore, Maryland 21218	10. PROGRAM ELEMENT, PROJECT, TASK AREA & WORK UNIT NUMBERS	
11. CONTROLLING OFFICE NAME AND ADDRESS Naval Sea Systems Command Washington, D.C. 20362 SEA05R15, Dr. H. H. Vanderveldt	12. REPORT DATE July 1981	
14. MONITORING AGENCY NAME & ADDRESS (if different from Controlling Office) David Taylor Naval Ship R&D Center Ship Materials Engineering Department Annapolis, Md. 21402	13. NUMBER OF PAGES 59	
16. DISTRIBUTION STATEMENT (of this Report) Approved for public release, distribution unlimited.	15. SECURITY CLASS. (of this report) Unclassified	
17. DISTRIBUTION STATEMENT (of the abstract entered in Block 20, if different from Report)	15a. DECLASSIFICATION/DOWNGRADING SCHEDULE	
18. SUPPLEMENTARY NOTES		
19. KEY WORDS (Continue on reverse side if necessary and identify by block number) acoustic emission piezoelectric transducer interferometer(optical probe) capacitive transducer deformation mechanisms		
20. ABSTRACT (Continue on reverse side if necessary and identify by block number) This report is a summary of research activities performed for the Naval Sea Systems Command (SEA 05R15) and the David Taylor Naval Ship Research & Development Center (Code 28) under Contract N00024-80-C-5337. The purpose of the present research is to use innovative optical techniques and superior signal capture and processing systems to determine the waveforms, frequency spectra, and propagational behavior of the acoustic emission signals		

unclassified

SECURITY CLASSIFICATION OF THIS PAGE (When Data Entered)

generated by the various mechanical deformation mechanisms leading to failure of metal alloys of prime importance to naval structures. The ultimate goal of this research is to absolutely determine the degree to which precise characterization of the acoustic emission signals can serve to remotely assess the severity of mechanical damage and give early warning of impending failure. Experiments were performed using a modified piezoelectric transducer, a Fizeau type interferometer, and a modified Michelson interferometer. Acoustic emission events were generated by pulling microtensile specimens in an extremely quiet microtensile machine and by the brittle, step unloading fracture of glass capillary tubes on the surface of test specimens possessing different geometries. All acoustic emission event waveforms were recorded by a high speed transient recorder and stored on magnetic mini-diskettes for analysis on a high speed digital computer and for future propagational behavior and waveform analysis. Specimens which were pulled on the microtensile machine were examined under optical and scanning electron microscopes to determine a point by point correlation between acoustic emission events and microstructural changes.



unclassified

SECURITY CLASSIFICATION OF THIS PAGE (When Data Entered)

Acoustic Emission Determination of Deformation
Mechanisms Leading to Failure of Naval Alloys

ANNUAL REPORT
(January 1980-December 1980)
Contract No. N00024-80-C-5337

July 1981

Prepared by: J. T. Glass, S. Majerowicz, R. E. Green, Jr.
Materials Science and Engineering Department
The Johns Hopkins University
Baltimore, MD 21218

Prepared for: Naval Sea Systems Command (SEA 05R15)
and
David Taylor Naval Ship R&D Center (Code 28)

DTNSRDC Report SME 81-44

Approved for public release; distribution unlimited

TABLE OF CONTENTS

	<u>Page</u>
ABSTRACT	iii
LIST OF ILLUSTRATIONS	v
INTRODUCTION	1
THEORETICAL CONSIDERATIONS	4
EXPERIMENTAL CONSIDERATIONS	6
ACOUSTIC EMISSION SOURCE IDENTIFICATION	12
OPTICAL DETECTION OF EMISSION SIGNALS	16
ACOUSTIC EMISSION SIGNAL CAPTURE AND PROCESSING	18
VERIFICATION OF SOURCE	19
RESEARCH PROGRESS DURING PHASE I	26

ACOUSTIC EMISSION DETERMINATION OF DEFORMATION MECHANISMS
LEADING TO FAILURE OF NAVAL ALLOYS

J. T. Glass, S. Majerowicz, and R. E. Green, Jr.
Materials Science & Engineering Department
The Johns Hopkins University
Baltimore, Md. 21218

ABSTRACT

This report is a summary of research activities performed for the Naval Sea Systems Command (SEA 05R15) and the David Taylor Naval Ship Research & Development Center (Code 28) under Contract N00024-80-C-5337. The purpose of the present research is to use innovative optical techniques and superior signal capture and processing systems to determine the waveforms, frequency spectra, and propagational behavior of the acoustic emission signals generated by the various mechanical deformation mechanisms leading to failure of metal alloys of prime importance to naval structures. The ultimate goal of this research is to absolutely determine the degree to which precise characterization of the acoustic emission signals can serve to remotely assess the severity of mechanical damage and give early warning of impending failure. Experiments were performed using a modified piezoelectric transducer, a Fizeau type interferometer, and a modified Michelson interferometer. Acoustic emission events were generated by pulling microtensile specimens in an extremely quiet microtensile machine and by the brittle, step unloading fracture of glass capillary tubes on the surface of test specimens possessing different geometries. All

acoustic emission event waveforms were recorded by a high speed transient recorder and stored on magnetic mini-diskettes for analysis on a high speed digital computer and for future propagational behavior and waveform analysis. Specimens which were pulled on the microtensile machine were examined under optical and scanning electron microscopes to determine a point by point correlation between acoustic emission events and microstructural changes.

LIST OF ILLUSTRATIONS

<u>Figure</u>	<u>Title</u>	<u>Page</u>
1	TYPICAL ACOUSTIC EMISSION WAVEFORMS	3
2	MODEL OF ACOUSTIC EMISSION SOURCES	6
3	MORE REALISTIC MODEL OF ACOUSTIC EMISSION SOURCES	6
4	ACOUSTIC EMISSION COUNT RATE AND STRESS VERSUS STRAIN GRAPHS	11
5	PIEZOELECTRIC SENSOR RESPONSES	13
6	EFFECT OF DETECTOR DISCRIMINATOR THRESHOLD VOLTAGE ON ACOUSTIC EMISSION COUNT RATE	14
7	THEORETICAL SURFACE DISPLACEMENT VERSUS TIME RECORD FOR A STEP-FUNCTION LOAD APPLIED TO AN INFINITE HALF SPACE	21
8	CAPACITIVELY MEASURED SURFACE DISPLACEMENT CAUSED BY A VERTICAL STEP-FUNCTION FORCE ON THE SURFACE OF A LARGE FLAT BLOCK	22
9	CAPACITIVELY MEASURED SURFACE DISPLACEMENT CAUSED BY STEP-FUNCTION FORCE; SEVERAL MILLISECOND TIME RECORD	24
10	COMPARISON OF OPTICALLY AND PIEZOELECTRICALLY DETECTED WAVEFORMS	25
11	LONGER TIME RECORDS, 2 msec, OF SAME WAVEFORMS IN FIG. 10	26
12	EFFECT OF SPECIMEN GEOMETRY ON A WAVEFORM AND ITS SPECTRUM	28
13	GEOMETRY USED IN THEORETICAL CALCULATIONS	30
14	THEORETICAL RADIAL SURFACE DISPLACEMENT RECORDS FOR $\theta = 30^\circ$ (SEE FIGURE 13)	31, 32
15	DIMENSIONAL DRAWING OF MICROTENSILE SPECIMEN USED IN ACOUSTIC EMISSION INVESTIGATION	34
16	SCHEMATIC OF PNEUMATIC TENSILE TEST MACHINE LOAD FRAME	37

<u>Figure</u>	<u>Title</u>	<u>Page</u>
17	SCHEMATIC OF PNEUMATIC TENSILE TEST MACHINE ACTUATOR CROSS-HEAD	38
18	SCHEMATIC OF FIZEAU INTERFEROMETER	39

INTRODUCTION

Acoustic emission or stress wave emission is the phenomenon of transient elastic wave generation due to a rapid release of strain energy caused by a structural alteration in a solid material. Generally these structural alterations are a result of either internally or externally applied mechanical or thermal stress. Depending on the source mechanism, acoustic emission signals may occur with frequencies ranging from several hertz up to tens of megahertz. Often the observed acoustic emission signals are classified as one of two types: burst and continuous. As shown in Fig. 1, the burst type emission waveform resembles a damped oscillation, while the continuous type emission appears to consist of an overlapping sequence of individual bursts. The importance of acoustic emission monitoring lies in the fact that proper detection and analysis of acoustic emission signals can permit remote identification of source mechanism and the associated structural alteration of solid materials. This information, in turn, can augment understanding of material behavior, can be used as a quality control method, and as a nondestructive evaluation technique for assessing the structural integrity of materials under service conditions.

There are a variety of sources of acoustic emission signals ranging from atomic size microstructural alterations to gross macrostructural changes such as earthquakes. A partial listing of reported sources includes movement of dislocations and grain boundaries; formation and growth of twins, crazes, microcracks,

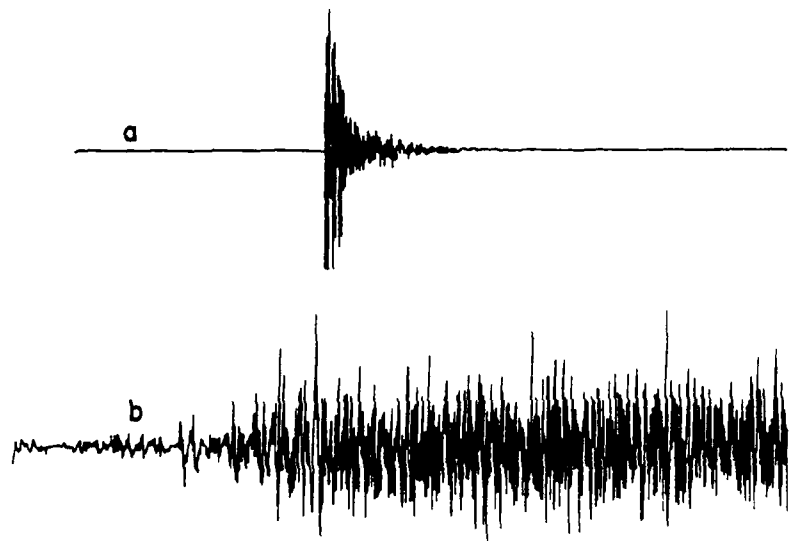


Fig. 1. Typical acoustic emission waveforms as detected with piezoelectric transducers, 4 msec time records: (a) burst type, (b) continuous type.

and cracks; stress-corrosion cracking; fracture of brittle inclusions and surface films; fiber breakage and delamination of composites; phase transformations; microseismic and seismic activity in geologic materials.

Although the phenomenon of acoustic emission has been the subject of an ever increasing number of scientific investigations and technological applications for more than 25 years (1-9), it has not optimally fulfilled its promise as a nondestructive testing technique since the waveforms, frequency spectra, and propagational characteristics of the stress waves emitted from specific defects remain unknown. The two major reasons for this state of affairs are oversimplistic, unrealistic theoretical models and lack of independently verified reproducible experimental measurements.

The purpose of the present research is to use innovative optical techniques and superior signal capture and processing systems to determine the waveforms, frequency spectra, and propagational behavior of the acoustic emission signals generated by the various mechanical deformation mechanisms leading to failure of metal alloys of prime importance to naval structures. The ultimate goal of this research is to absolutely determine the degree to which precise characterization of the acoustic emission signals can serve to remotely assess the severity of mechanical damage and give early warning of impending failure.

THEORETICAL CONSIDERATIONS

Figure 2 serves to illustrate the oversimplistic manner in which acoustic emission is usually treated theoretically. Acoustic emission signals propagating away from internal and surface sources are detected by a transducer located on the surface of the test piece. In this commonly used portrayal, the internal source emits a single compressional spherical wave which propagates at constant velocity in all directions. Its amplitude decreases inversely with distance from the source only because of the expanding wavefront so that the total energy contained in the wave remains constant. The surface source also emits a single compressional spherical wave with similar characteristics from the crack tip, and in addition, emits a Rayleigh wave which propagates along the surface in all directions away from the source with constant velocity. The surface wave amplitude decreases as the square root of the distance from the source only because of the expanding wavefront.

Figure 3 illustrates schematically a somewhat more realistic view of acoustic emission, although even this portrayal is still oversimplified. The internal source emits a wave which is non-spherical initially because of the source shape. After leaving the source, the profile of the wavefronts continue to change because of the directional variation in wave velocities associated with linear elastic wave propagation in anisotropic solids. Moreover, the amplitude of the wave decreases with increasing

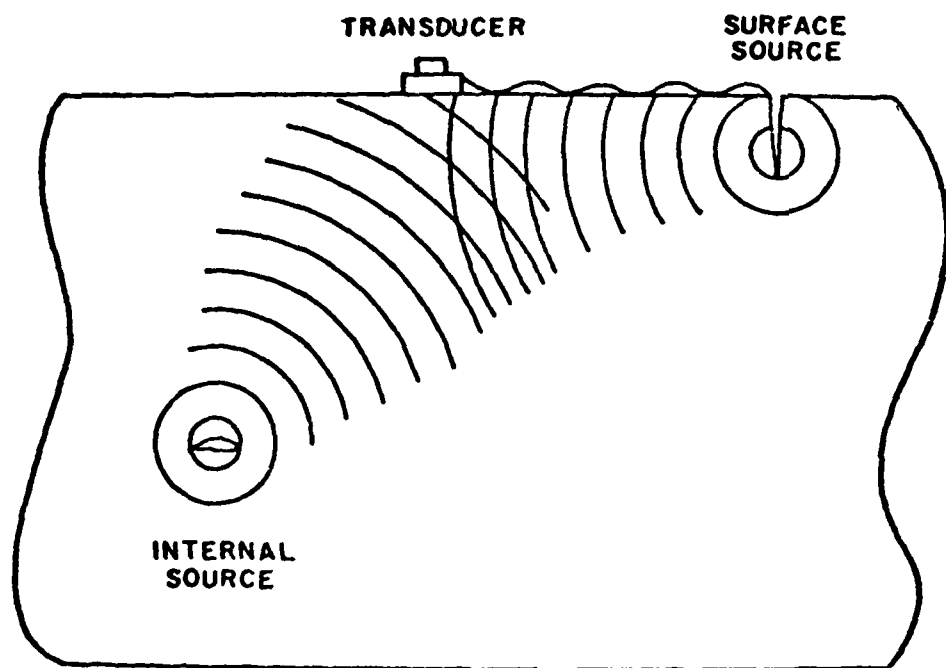


Fig. 2. Oversimplified model of acoustic emission sources.

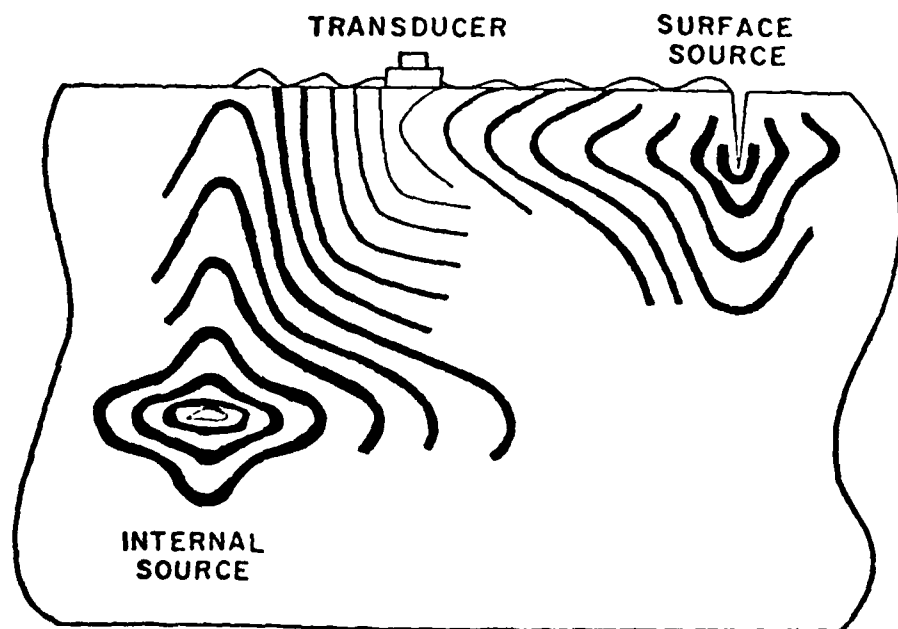


Fig. 3. More realistic simplified model of acoustic emission sources.

distance from the source, both as a result of the expanding wavefronts and as a result of attenuation caused by a number of mechanisms which absorb and scatter elastic waves in real materials. Among these mechanisms are thermoelastic effects, dislocation damping, subgrain and grain scattering, and interaction with ferromagnetic domain walls.

Other factors which also influence the acoustic emission signals detected on the surface of real materials include the fact that actual sources may emit both longitudinal and shear waves which possess a distribution of frequencies and amplitudes. Even in a single direction, these waves can propagate with different wave speeds, and the higher frequency components experience stronger attenuation than the lower frequency components. Moreover, the elastic waves experience diffraction (beam divergence) and refraction (energy-flux deviation), mode conversion at internal and surface boundaries, and those with sufficient amplitude will be subject to non-linear effects.

EXPERIMENTAL CONSIDERATIONS

The most simple type of acoustic emission detection system commonly used consists of a piezoelectric transducer directly attached to the workpiece with an acoustic impedance matching coupling medium. The voltage output from the transducer is fed directly into a preamplifier, which is located as close to the transducer as possible. The preamplifier output signal is then passed through a variable bandpass filter to a main amplifier connected to a signal analysis system, which produces an analog

or digital signal every time the amplified acoustic emission voltage signal exceeds a selected discriminator threshold level. The most frequently used method for evaluating structural damage by acoustic emission monitoring is to count the signals emitted during deformation of the material and to plot the results as count rate or total count as a function of some measure of the deformation such as pressure, stress, strain, or number of fatigue cycles. Several problems are associated with this simplistic approach including a lack of knowledge of the influence of test specimen geometry on the received signals, of the effect of the medium coupling the transducer to the workpiece, the amplitude and frequency response of the transducer, resonances in the active element and other components of the transducer, and the electronic system used to select, filter, transmit, and amplify the signals. In order to make reliable assessment of such data, it is normally assumed that all events producing acoustic emissions of sufficient amplitude to be counted are equally damaging to the structure, that all damaging events will produce acoustic emissions of sufficient amplitude to be counted, and that each event will cause an acoustic emission which will be counted only once and not overlap with other signals. To make such assumptions is improper since a given high amplitude acoustic emission signal may be produced by a single event which causes damage to the structure or by simultaneous occurrence of a number of small events which cause no structural damage but

whose net effect is to produce the large acoustic emission signal. A structurally damaging event may occur, but the emissions associated with it may be too weak, propagate away from the detecting transducer, or be of the wrong frequency to be detected. A single event may take place with several emissions of sufficient amplitude that the detector records several counts for one event, or a single event may be such that the direct signal and reflected signals arrive at the detecting transducer at different times thus resulting again in multiple counts from a single event.

Other methods used to process acoustic emission signals are to record the mean-square voltage, which is a measure of the energy content, and the root-mean-square voltage, which is a measure of the signal amplitude. In order to locate the source of an acoustic emission event, it is customary to arrange a number of transducers in a prescribed geometrical pattern on the workpiece. A computer controlled signal analysis system is programmed to compare arrival times of acoustic emission signals at the individual transducers and to combine this information with known wave velocities to locate the source.

A review of the literature reveals many experiments where the detection technique did not permit recording of the unaltered acoustic emission signal characteristic of the structural defect or microstructural alteration. In other experiments proper precautions were not taken to eliminate signals caused by extraneous noise sources. In most cases where the observed

acoustic emission signals were assumed to be caused by a given microstructural alteration, no metallographic or other independent evidence was presented to verify the assumption.

Figure 4(a), taken from the original work of Dunegan and Harris, (10) serves as a prime example of a case where the results of a single experiment have been republished over and over again in the literature in such a fashion that the unwary reader is led to believe that the results shown represent a well-established agreement between acoustic emission measurements and theory. Figure 4(a) shows graphs of acoustic emission count rate and stress plotted as a function of strain for a 7075-T6 aluminum tensile specimen. The dashed curve superimposed on the acoustic emission data is a fit of Gilman's mobile dislocation model as a function of strain. Indeed, the agreement between theory and experiment is excellent. However, the fact that this agreement is not typical is not mentioned in the vast majority of re-publications of this figure, although this fact is clearly brought out by Dunegan and Harris in their original paper: "The results of this excellent fit of Gilman's equation to our data was very encouraging until other materials were tested and a fit attempted." Figure 4(b), also taken from their paper, shows the same set of graphs for an iron-3% silicon tensile specimen. It was impossible to obtain any fit whatsoever to Gilman's theory in this case.

The fact that Fig. 4(a) shows agreement between acoustic emission count rate and mobile dislocation density theory is

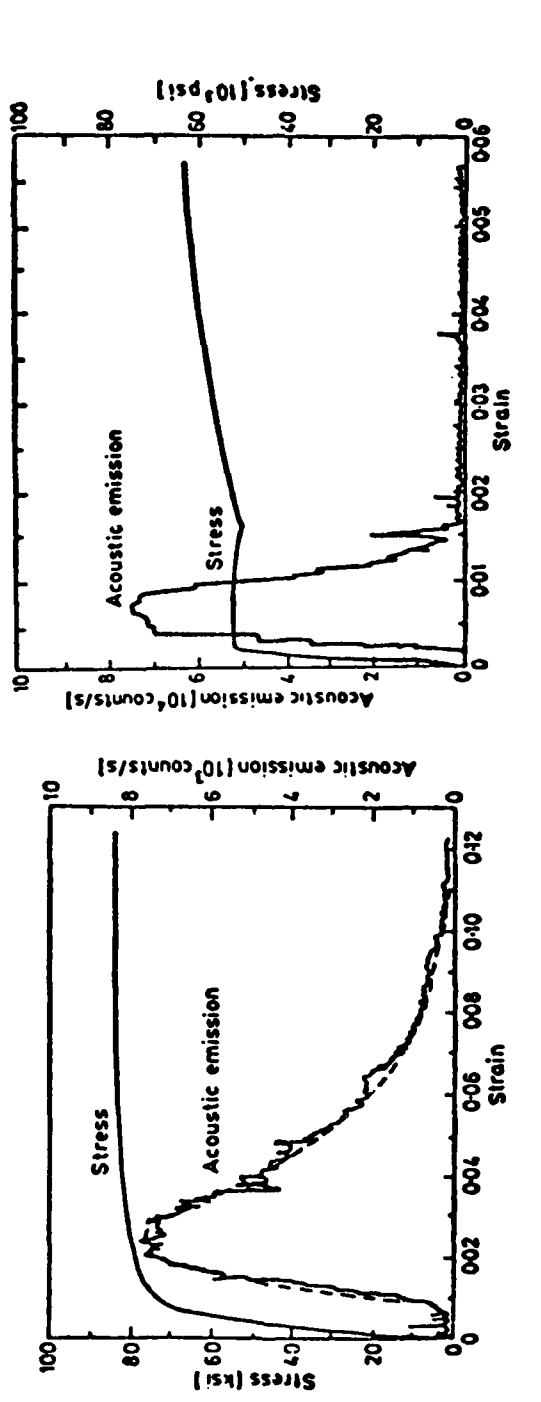


Fig. 4. Acoustic emission count rate and stress as a function of strain (after Dunegan and Harris(10)): (a) 7075-T6 aluminum, (b) Iron-3% silicon.

(b)

(a)

probably fortuitous since not only do different sensors respond differently to the same acoustic emission signal as shown in Fig. 5, but even for a fixed detection system the recorded acoustic count rate can be made to vary over a wide range depending on choice of the detector discriminator threshold voltage setting as shown in Fig. 6. Comparison of Fig. 6 with Figs. 4(a) and (b) shows that nearly any asymmetric distribution of acoustic emission count rate can be plotted experimentally, if the correct choice of detecting transducer and discriminator threshold is made. Thus, all such plots reported to date must be regarded with some skepticism.

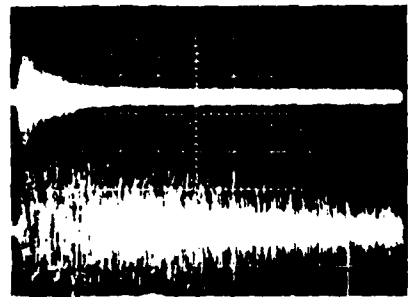
ACOUSTIC EMISSION SOURCE IDENTIFICATION

In order to positively identify the source of an acoustic emission signal and hence be able to make a definitive statement as to whether or not the material alteration causing the acoustic emission signal is harmful to the integrity of the engineering structure, it is necessary to be able to determine the unmodified waveform and frequency spectrum of the signal itself. Moreover, once this determination is made, one must be able to compare the characteristics of the acoustic emission signal in question with a previously characterized set of acoustic emission signals recorded from known material defects.

Prior to recent research at the National Bureau of Standards and the Johns Hopkins University no reliable method had been developed to solve the acoustic emission characterization



SHEAR SENSOR
1.7 MHz
EDGE MOUNTED
GAIN OF 100
HI-PASS FILTER-1.2 MHz
0.05 VOLTS/CM
0.001 SEC/CM



ULTRASONIC SENSOR
1 MHz CUT, SURFACE MOUNT
GAIN OF 100
HI-PASS FILTER-600 kHz
0.01 VOLTS/CM
0.001 SEC/CM

ACCELEROMETER
ENDEVCO #2213E, SURFACE MOUNT
GAIN OF 100
HI-PASS FILTER-30 kHz
0.05 VOLTS/CM
0.001 SEC/CM

Fig. 5. Different piezoelectric sensor responses to the same acoustic emission signal (after Hutton and Ord[1]).

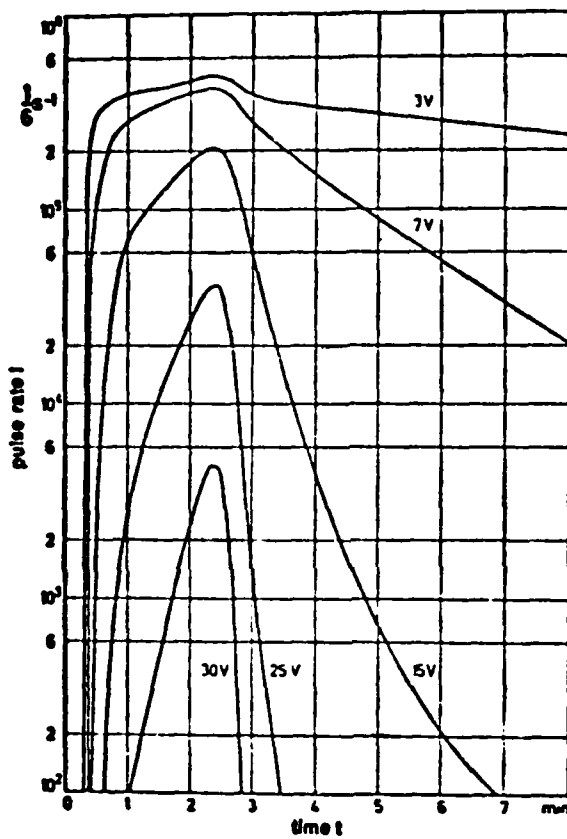


Fig. 6. Influence of detector discriminator threshold voltage setting on shape of acoustic emission count rate versus time curve for the same acoustic emission signal and piezoelectric transducer (after Jax and Eisenblattér[11]).

problem. In fact, numerous investigators have gone on record in the published literature as calling the problem "unsolvable." The major reason for such a pessimistic view is that there are several difficulties which must be overcome in order to reliably characterize acoustic emission signals.

First, a detector system must be used which is capable of sensing surface displacements due to both internal and surface acoustic emission sources which does not modify the signal because of its own limitations. Although they have been used in the past, and are still the detectors most often used in current practice, conventional piezoelectric transducers are completely unsuited for such measurements since they have their own amplitude, frequency, and directional response. In addition, they "ring" at their resonance frequency and it is impossible to distinguish between the amplitude (voltage output) excursions caused by this "ringing" and the amplitude variations actually characteristic of the acoustic emission source. Also, piezoelectric transducers must be coupled to the workpiece with a material which possesses a suitable acoustical impedance match and, consequently, the waves being measured are physically disturbed. Finally, it is uncertain just what a piezoelectric transducer actually measures; commercial piezoelectric transducers are known to vary markedly in their performance characteristics; and the performance characteristics which they possess when initially purchased are known to alter detrimentally in time.

The second difficulty is to accurately determine the acoustical transfer characteristics of the workpiece. If we assume that we do have an ideal detector of surface displacements, then the question still remains as to how these surface displacements relate to the displacements of the material at the internal or distant surface source of the acoustic emission signals. The need is for the transfer function which describes how a known source signal is modified by the propagational characteristics of the material as the elastic waves leave the source and pass through a solid body of prescribed geometry. Determination of this transfer function is a necessity in order to answer the real question which is the inverse problem. Assuming that all surface displacements are accurately known, and the direct transfer function also known, one can then solve the inverse problem of source displacement determination and hence identify the source mechanism and assess its influence on the structural integrity of the workpiece.

Considerable progress in acoustic emission waveform determination was made by Breckenridge et al.(12) who developed a method for obtaining the waveforms of simulated acoustic emission sources which were unmodified by ringing of the specimen and transducer. Their technique was based on the comparison of two signals at the transducer, one from the event in question and one from an artificial event of known waveform. For the standard-source event they chose a step

function of stress which was realized experimentally by fracturing a glass capillary at the center of one flat surface of a large cylindrical aluminum alloy transfer block. In order to have a broadband detector they used a dc-biased capacitive transducer with an air-gap dielectric. They found that measurements of the waveform, both on the same surface as the source and on the opposite surface yielded results that agreed remarkably well with theoretical predictions. An important conclusion from their work was that no difference was observed between the shape of the vertical displacement at the epicentral point produced by a source event on the surface and that produced by a similar event in the interior of a solid.

Subsequently, Hsu et al. (13,14) numerically computed the displacement as a function of time at an arbitrary point on an infinite plate due to a point source fource function. Nearly perfect experimental agreement with their theory was obtained by using a reproducible step-function stress release pulse as a simulated acoustic emission signal and a wide band capacitive transducer as a sensor.

OPTICAL DETECTION OF ACOUSTIC EMISSION SIGNALS

In order to optimally solve the detector problem several laser beam optical systems for detection of acoustic emission signals have been developed (15-32). These optical detectors offer many important advantages over piezoelectric transducers for monitoring acoustic emission events. Among these advantages

are: direct contact with the test specimen is unnecessary; no acoustical impedance matching couplant is required; the waveform and frequency spectrum of the acoustic emission event is not modified by the optical probe; optical probes have inherent broad flat frequency responses; they can probe internally in transparent media; they can be used to make measurements on extremely hot and extremely cold materials and in other environments hostile to piezoelectric transducers; since the focused laser beam diameters are typically only a few hundredths of a millimeter, they can probe very close to a slip band, mechanical twin, included particle, crack, or other material defect.

An optical acoustic emission detector can be used as a point probe to measure the waveforms directly at the site of an internal source in a transparent solid. It can be used to measure the waveforms as a function of position in the solid as well as on its surface. Thus correlation can be achieved between the acoustical characteristics of the source and the detected surface signals. A laser beam acoustic emission detector system completely solves the aforementioned detector difficulty and permits progress to be made on the transfer function problem.

Optical probes have already been used to measure mechanical twinning of cadmium, indium, tin, and zinc; cracking of glass by both thermal and mechanical means; stress-corrosion cracking in E4340 steel and 7039 aluminum; allotropic transformation

in iron; and plastic deformation and fracture of 304L stainless steel.

ACOUSTIC EMISSION SIGNAL CAPTURE AND PROCESSING

Conventional procedures for capturing acoustic emission waveforms and subsequent processing, such as Fourier analysis in order to determine the frequency spectrum, usually involve use of a "broadband" piezoelectric transducer, a video tape recorder, and a commercially available spectrum analyzer(33). The gross deficiencies of piezoelectric transducers for this purpose have already been enumerated and will be illustrated by a specific example in the next section. Although a video tape recorder has proven to be an economical method of almost continuous recording of acoustic emission signals over time periods as long as several hours, it is not an optimum device for faithful recording and reproduction of acoustic emission waveforms. It has limited bandwidth (4 MHz), clips negative signals more than positive ones, and requires use of a gate in order to remove signal artifacts due to synchronization pulses internally generated by the recorder and alternation of the video recording heads.

The best system currently available for reliable recording and reproduction of individual acoustic emission waveforms is a transient recorder which has a high digitizing speed and a long time window coupled to a digital magnetic disc or tape recorder. The magnetically stored signal serves as input to a high speed digital computer for signal processing including

fast Fourier transforms for spectral analysis(26,28).

VERIFICATION OF SOURCE IDENTIFICATION SYSTEM CAPABILITY

In order to assure that a selected experimental acoustic emission source identification system can be successfully used to detect and record the unknown waveforms of acoustic emission signals characteristic of real structural or micro-structural materials alterations, it must first be shown that the system is capable of faithful detection and recording of waveforms produced under carefully controlled experimental conditions which correspond to known theoretical waveform solutions.

Although this has been successfully accomplished using capacitative transducers(12-14) and optical detectors(26-29), there has not been a single case of such an accomplishment using piezoelectric transducers.

Figure 7 shows the theoretically computed vertical surface displacement versus time record for a step-function time dependence point source load applied to the surface of a homogeneous isotropic linear elastic half-space. As mentioned previously, Breckenridge et al.(12) used a capacitive transducer to measure the vertical surface displacement due to a rapid unloading pulse caused by fracture of a glass capillary tube against a specially designed test block. The results of this measurement, as can be seen reproduced in Fig. 8, show remarkable agreement with the theoretical predictions.

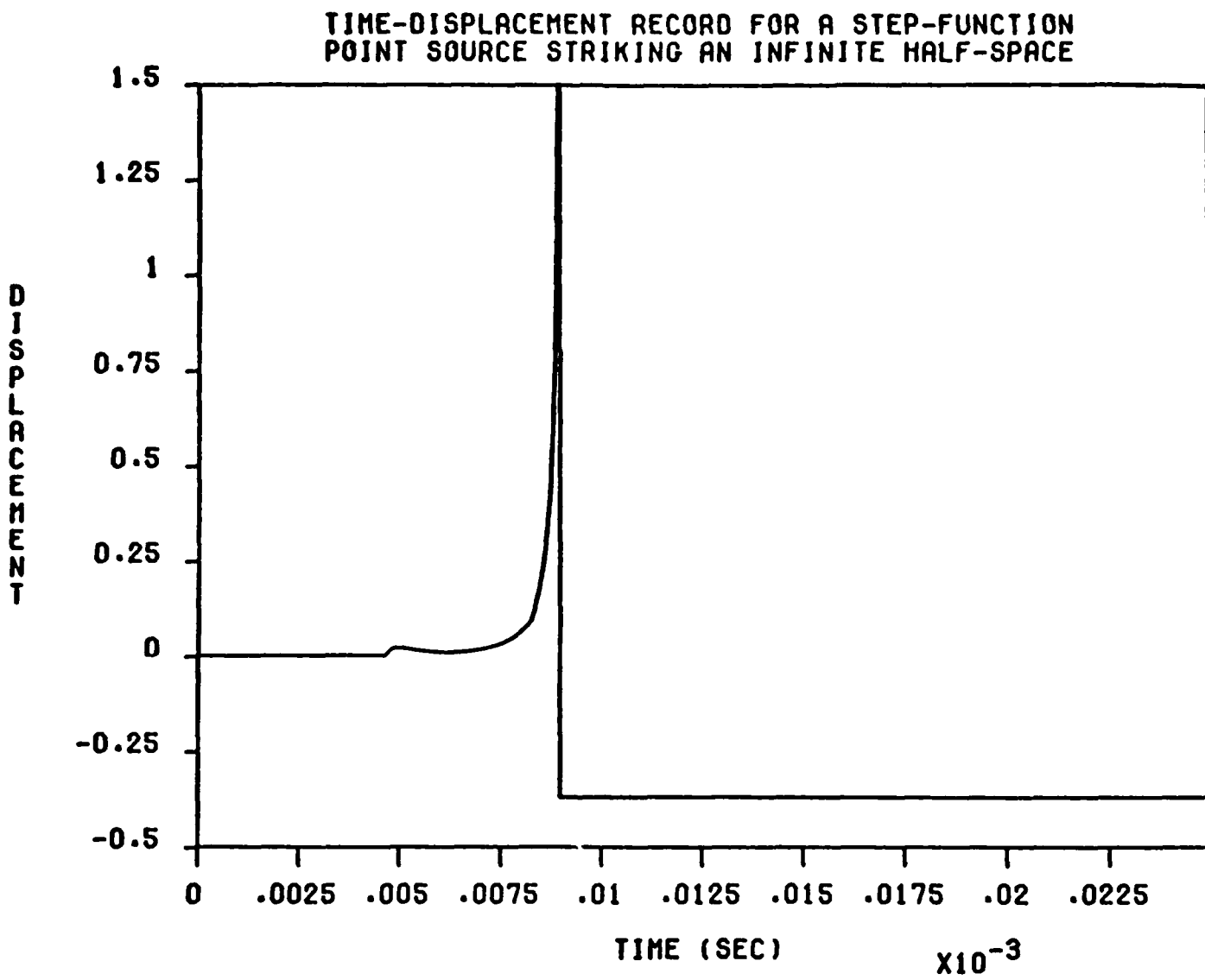


Fig. 7. Theoretical vertical surface displacement versus time record for a step-function time dependence point source load applied to the surface of a homogeneous isotropic linear elastic half-space.

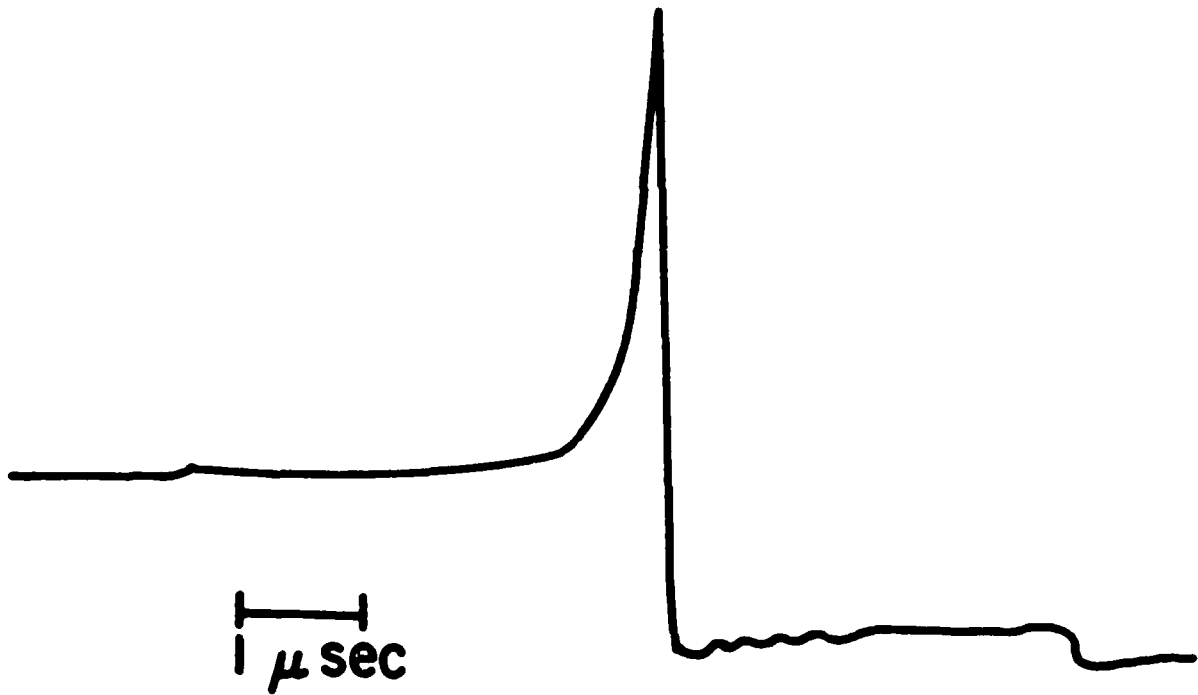


Fig. 8. Capacitively measured vertical surface displacement caused by a vertical step-function force on the surface of a large flat block. (after Breckenridge et.al.[12]).

When the surface displacement was measured over a longer time period of several milliseconds, the waveform shown in Fig. 9 was obtained. The actual waveform characteristic of the source can still be seen at the far left of the figure, while the subsequent large oscillations are deemed to be due to reverberations in the test block and support structure. Similar results were obtained by Hsu and Hardy (14) for epicenter displacements produced by breaking glass capillaries on an aluminum plate.

Figure 10 compares 200 μ sec waveforms from fracture of a glass capillary against an aluminum test block as detected (a) optically and (b) piezoelectrically. The portion of the optically detected signal to the left of the vertical dashed line agrees within experimental accuracy with theoretical predictions of the displacement associated with the source. An arrow indicates an enlarged view of this portion of the waveform. Even longer time records, 2 msec, of the same two waveforms are presented in Fig. 11. As can be seen in Figs. 10 and 11, the piezoelectric transducer introduces a multitude of oscillations into the detected waveform and does not faithfully reproduce the waveform due to surface displacements characteristic of the acoustic emission source.

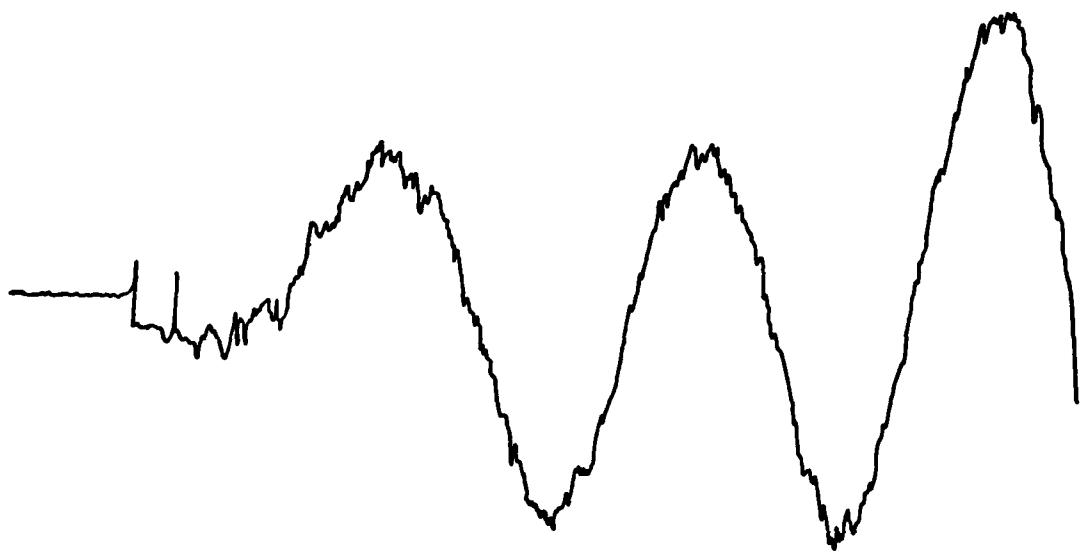


Fig. 9. Capacitive transducer measured vertical surface displacement due to fracture of glass capillary against aluminum test block, several millisecond time record (F. R. Breckenridge, private communication).

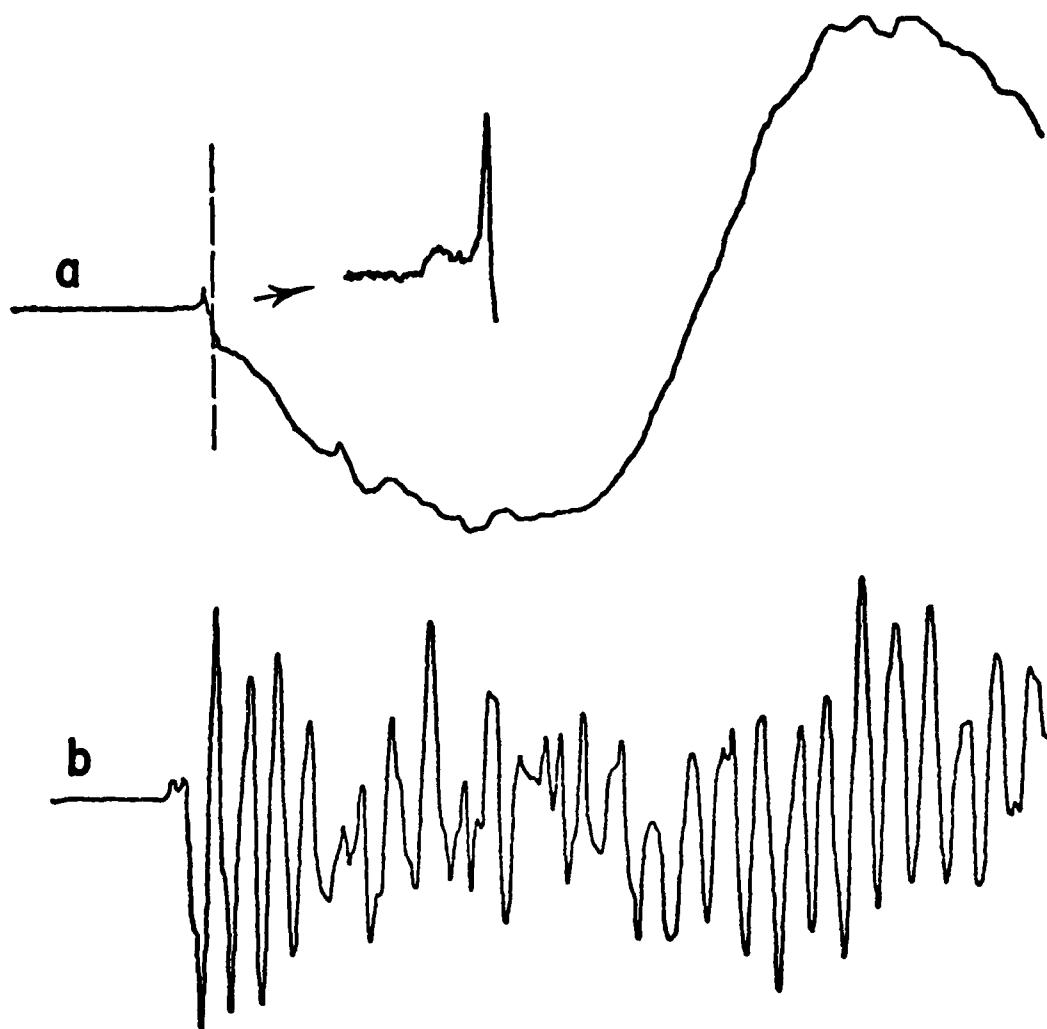


Fig. 10. Comparison of waveforms from fracture of a glass capillary as detected (a) optically and (b) piezoelectrically, 200 μ sec time records. The portion of the optically detected signal to the left of the vertical dashed line agrees with theoretical predictions of the displacement associated with the source. Arrow indicates enlarged view of this portion of waveform.
(after Djordjevic and Green[26]).

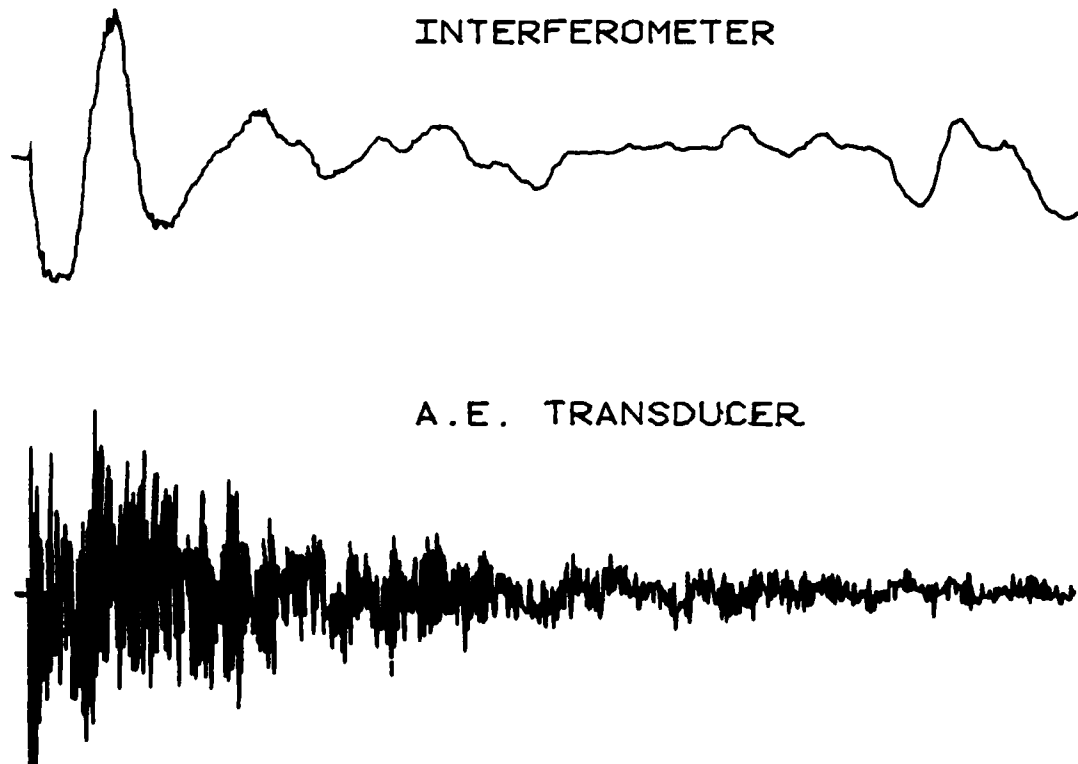


Fig. 11. Longer time records, 2 msec, of same two waveforms as shown in Fig. 10 (after Djordjevic(28)).

RESEARCH PROGRESS DURING PHASE I

As has been shown in the previous section, even when a capacitive transducer or optical probe is used to faithfully detect the surface displacement waveform characteristic of an acoustic emission source, the waveform, and hence the frequency spectrum, appears to undergo severe modification as it reflects back-and-forth inside an actual workpiece. In order to absolutely prove or disprove this hypothesis, it is necessary to compute theoretically the waveforms and frequency spectra to be expected from a variety of specific combinations of well-characterized sources and workpieces. It is desired to calculate the particle motion both inside and on the surface of a workpiece of known material and geometry as a result of a known applied force. A schematic illustration of this problem in which only the geometry of the workpiece is changed is shown in Fig. 12.

Weisinger (34) performed such a theoretical calculation for the case of a point source with step function force time dependence radially exciting the surface of a homogeneous, isotropic, linear elastic sphere. He used the normal mode technique to compute the eigenfrequencies and displacement eigenfunctions for the sphere. Combining these results with the given source model, the displacement for any point on or within the sphere was expressed analytically as a summation over all the discrete eigenfrequencies of the sphere.

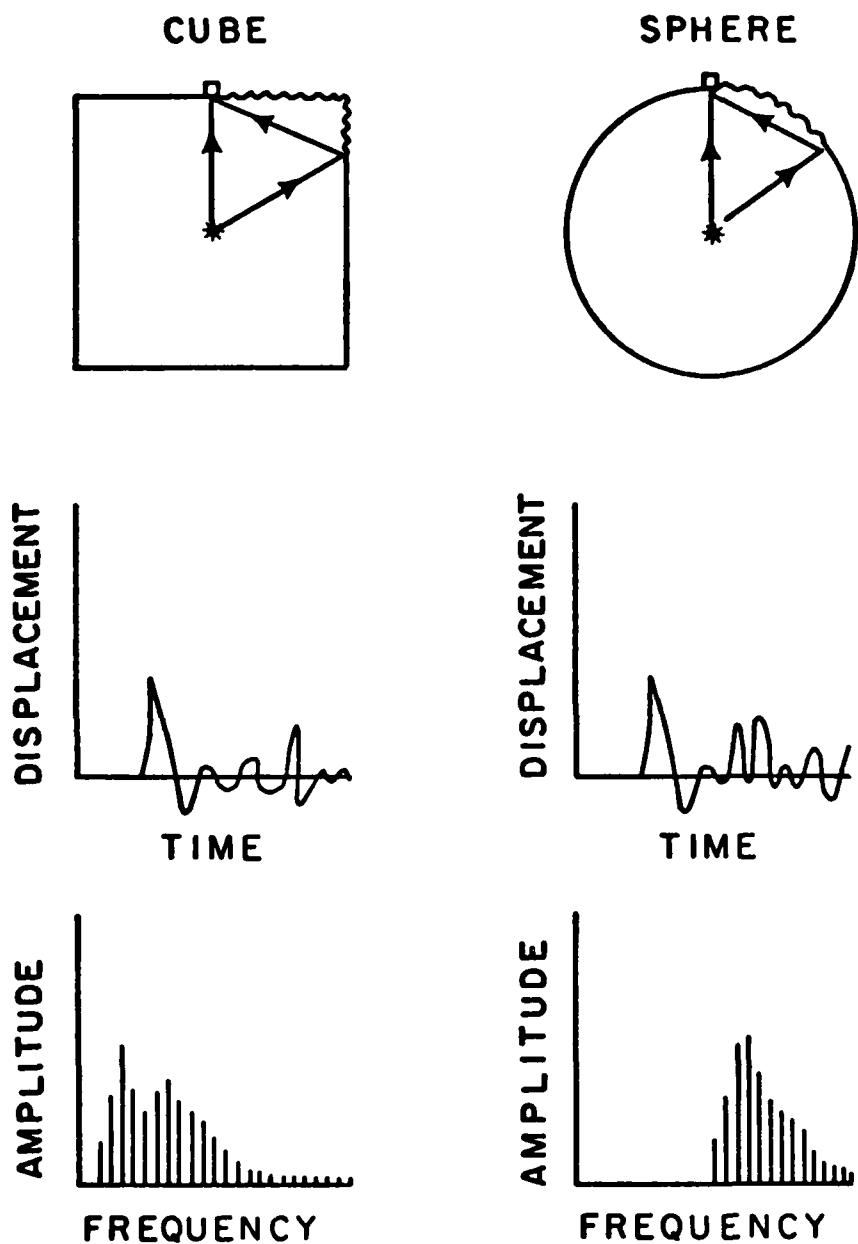


Fig. 12. Schematic illustration of waveform and frequency spectrum modification of acoustic emission signal due to specimen geometry (R. Weisinger, private communication).

Numerical calculations were performed for a steel sphere and displacement versus time records were plotted for various locations on the sphere's surface. At a given location both surface waves and body waves appeared in the displacement-time record; the arrival times of these waves agreed very well with those predicted by ray theory. Figure 13 shows the geometrical arrangement used to make the calculations, while Fig. 14 shows the results obtained for the radial surface displacement at an angle of 30° on a steel sphere caused by a step-function time dependent force acting at 0° . Figure 14(a) shows the early arrival time record for the first 25 microseconds and Fig. 14(b) shows the longer time record for 250 microseconds. P represents the arrival time for the first arriving compressional wave, S the arrival time for the first arriving shear wave, and R, the arrival time for the first arriving Rayleigh surface wave. Additional subscripts refer either to compressional (P_2, P_3) waves or shear (S_2, S_3) waves which have undergone multiple reflections inside the sphere without mode conversion. Notation such as PS refer to a compressional wave which has converted partially into a shear wave as a result of one reflection.

The results of these calculations suggest characteristics which may be common to all types of acoustic emission signals. The first signals to appear on the displacement-time record can be attributed primarily to the nature of the acoustic emission source, while later portions of the record are dominated by long period oscillations and body wave reflections caused by

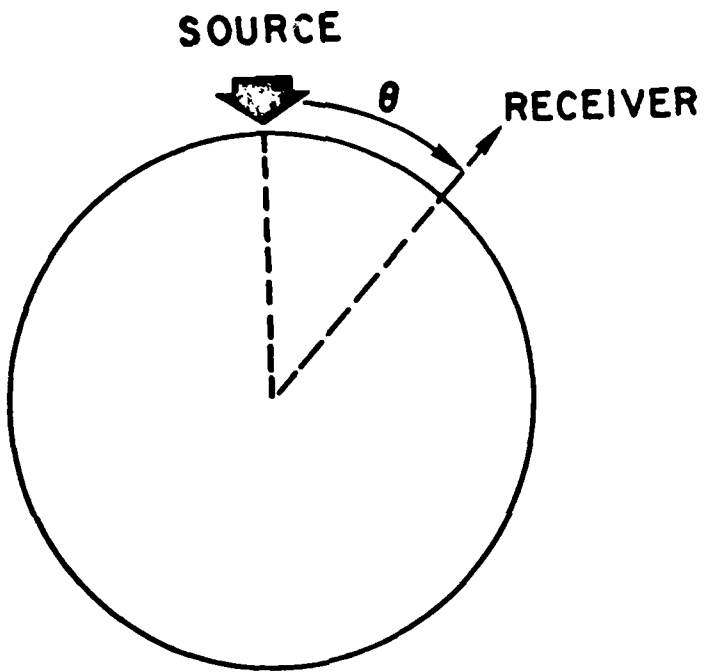


Fig. 13. Geometrical arrangement used to make calculations. Step-function time dependent force acting at 0° . Radial surface displacement measured at angle θ from source. (after Weisinger[34]).

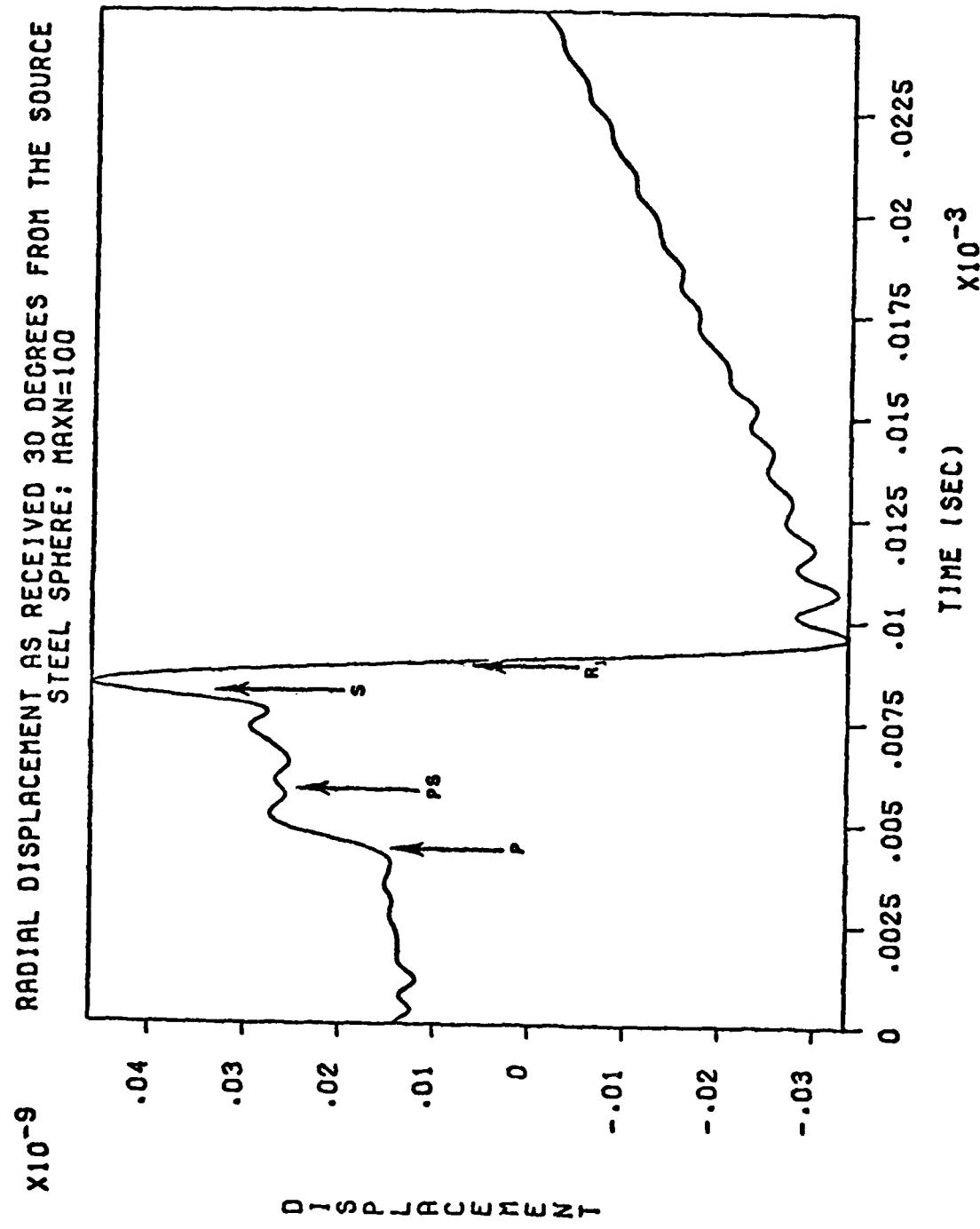


Fig. 14 (a). Early arrival time record showing the first 25 microseconds of the radial surface displacement at an angle of 30° on a steel sphere caused by a step-function time dependent force acting at 0° . (after Weisinger [34]).

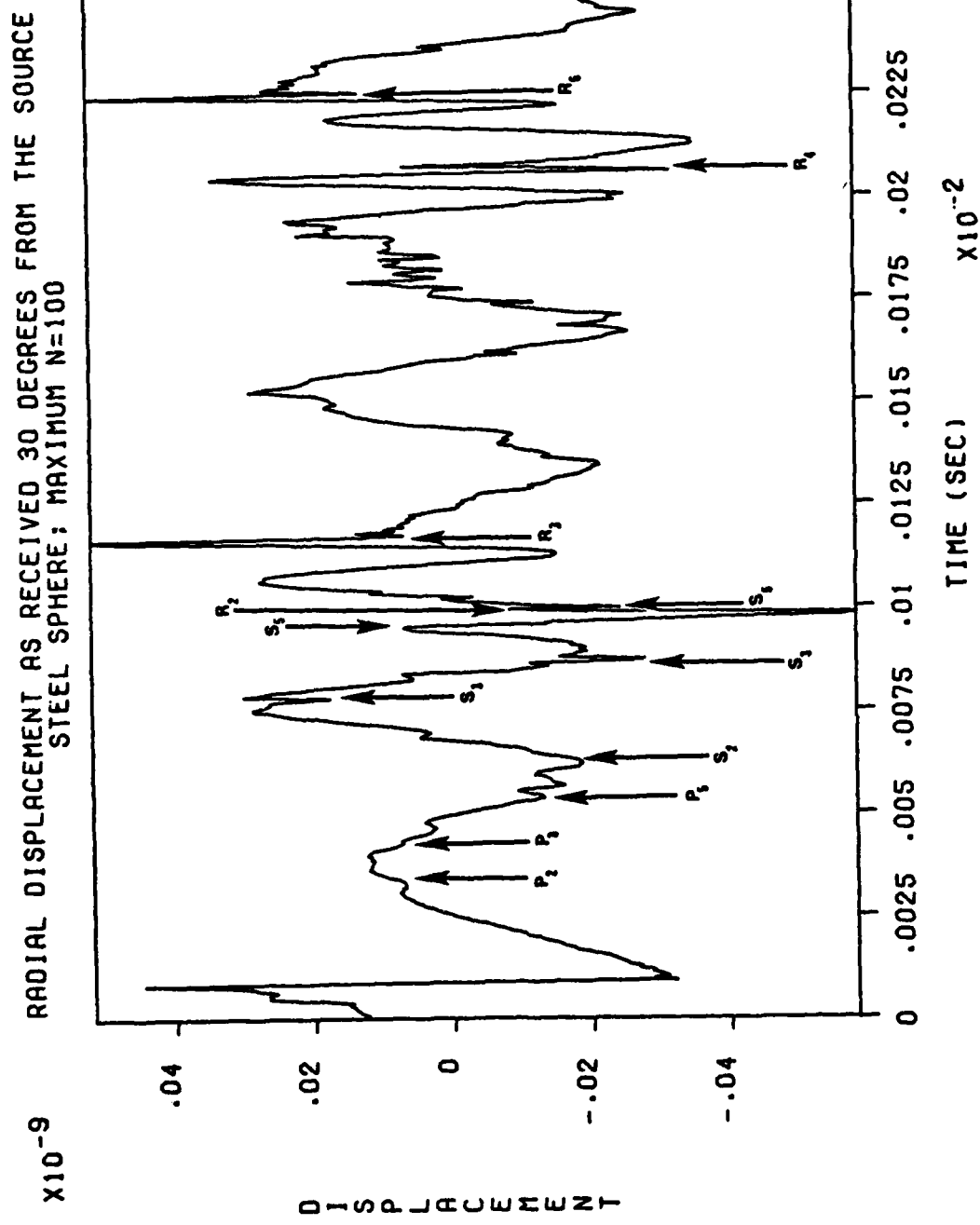


Fig. 14 (b). Longer time record showing 250 microseconds of the radial surface displacement at an angle of 30° on a steel sphere caused by a step-function time dependent force acting at 0° . (after Weisinger[34]).

both the nature of the source and the finite size of the specimen.

In order to assure that the acoustic emission signal detected at a location on the surface of the workpiece remote from the source is still representative of the source it is necessary to experimentally measure acoustic emission signals as close to the source as possible.

Although the literature is saturated with claims of acoustic emission source identification due to a variety of microstructural alterations in real materials, all of these measurements have been made on large specimens with piezoelectric transducers either located on the specimens at locations remote from the source or, even worse, located on specimen grips or other supports. It should be obvious from the considerations of the previous sections why such measurements must be viewed with skepticism.

In an effort to measure the acoustic emission signals as close to an actual microstructural alteration source as possible in a technically important material experiments were initiated with micro-tensile test specimens possessing very small gauge sections as shown in Fig. 15. This reduction in the volume of material from which acoustic emissions can be produced during tensile elongation offers the following advantages: permits placement of the optical probe extremely close to the source; reduces the number of potential sites for acoustic emission generation; reduces the overlap between signals since fewer will be generated; reduces the number of potential loss or

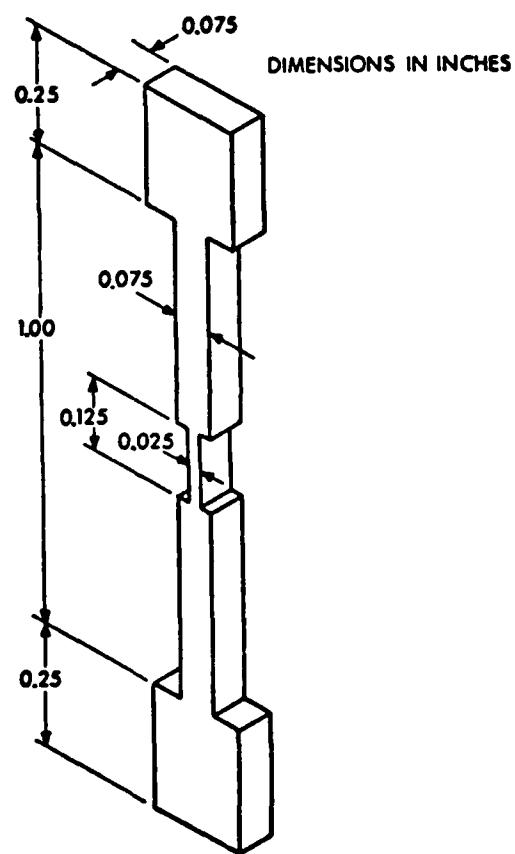


Fig. 15. Dimensional drawing of microtensile specimen
(after Bruchey [32]).

attenuation sites present.

Using 304L stainless steel specimens of this geometry, coupled with a laser beam optical probe, and an ultra-quiet pneumatic tensile load system, Bruchey(32) found that the specimens failed by void nucleation, growth, and coalescence. Although a full spectrum of material choices was considered ranging from single crystals to complicated engineering alloys, it was decided that an engineering alloy should be chosen since the ultimate goal of acoustic emission measurements is to inspect engineering structures under service conditions. 304L stainless steel was chosen because this material falls within the general category of austenitic stainless steels, which enjoy the greatest usage of all stainless steels.

As shown in Fig. 15, the micro-tensile specimen possesses T-shaped grip ends, a gauge section, and a sub-gauge section. During tensile elongation, plastic deformation is limited to this sub-gage section, which comprises a volume of material of about three cubic millimeters. Thus the sources of acoustic emission are localized and examination of the sub-gauge length surfaces by optical and scanning electron microscopy expedited. Since inaccurate machining of the test specimen can lead to misalignment problems and extraneous noise sources and since the specimens are extremely small, particular care was taken in specimen preparation. In addition to very careful machining, each specimen was individually mounted in a room temperature setting epoxy and given a fine metallographic polish. After

polishing, the epoxy was dissolved away chemically without damage to the test specimen.

A number of tensile test machines were investigated for use in elongation of the micro-tensile specimens but were rejected because excessive noise was generated by mechanical components or by fluid motion through valves, orifices, and pistons. This noise problem was overcome by use of a pneumatic tensile test machine which was modified to optimally test the micro-tensile specimens. A schematic drawing of the pneumatic tensile test machine load frame is shown in Fig. 16 and of the actuator crosshead in Fig. 17. The extreme quietness of this machine is due to the fact that there is no metal-to-metal contact to act as a noise source. The pistons are not in contact with the cylinder walls and piston-cylinder friction is kept to a minimum by the rolling piston seal.

Figure 18 shows a schematic diagram of the Fizeau interferometer used to measure the specimen surface displacements caused by the acoustic emission signals. An expanded laser beam is incident from the left and is focused by the lens on the specimen surface. Approximately half of the incident light is reflected by the beam splitter and focused on the reference mirror R. The two beams, one reflected from the specimen surface and one reflected from the reference mirror, are recombined at the beam splitter and produce a fringe pattern at the output which is focused on the photodetector.

The electrical signal output from the photodetector was fed into a 20 dB amplifier and then analog to digital conversion

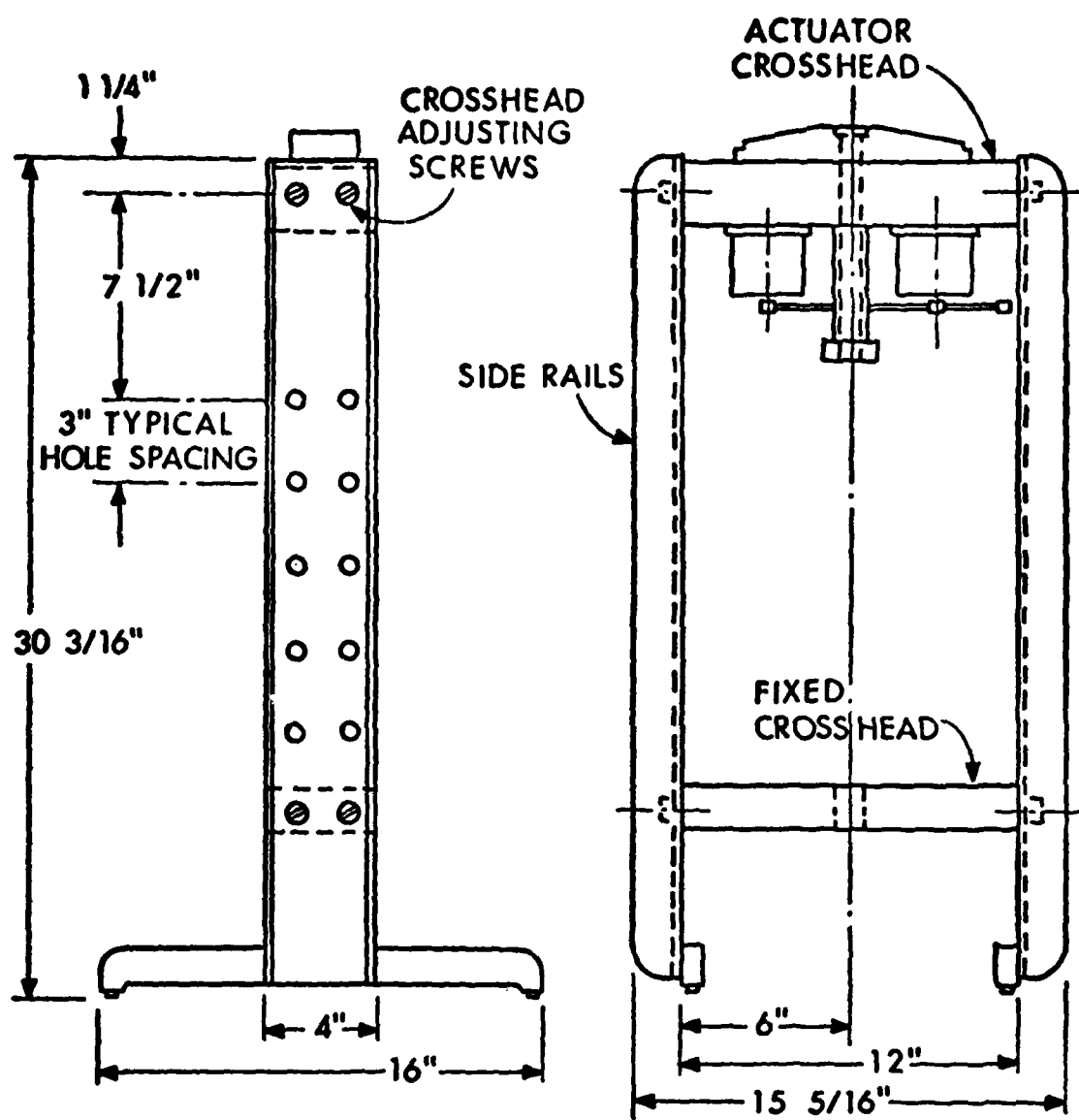


Fig. 16. Schematic of pneumatic tensile test machine load frame.

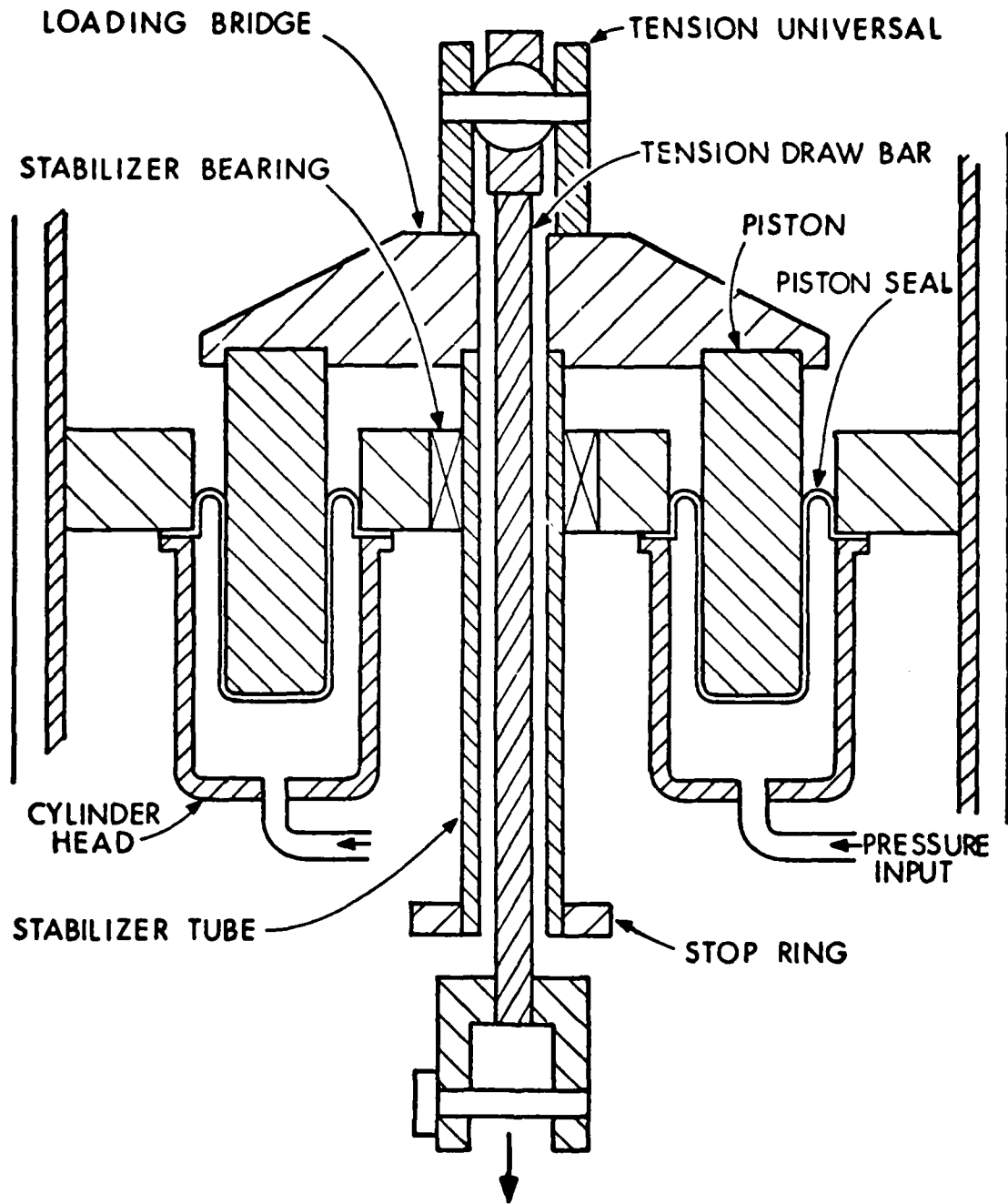


Fig. 17. Schematic of pneumatic tensile test machine actuator crosshead.

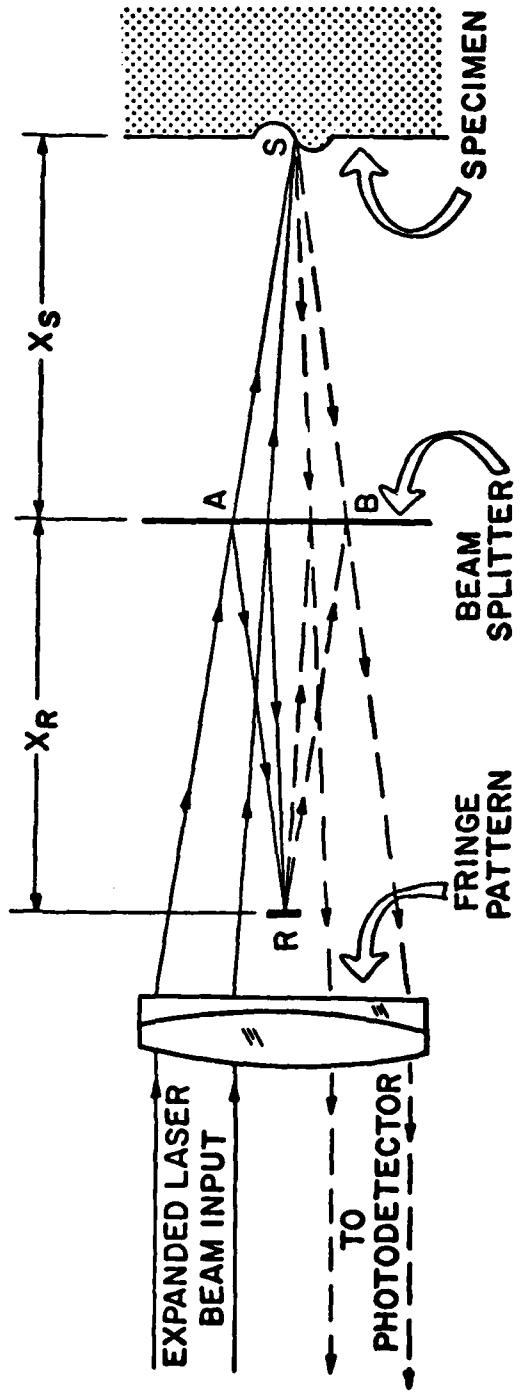


Fig. 18. Schematic of Fizeau interferometer used to detect acoustic emission signals. (after Palmer[27]).

was performed by a Nicolet Explorer III Digital Oscilloscope with a Model 204-2 Plug-in. This combination afforded the capability of recording up to 4096 points at a maximum rate of 50 nanoseconds per point at 8 bits of vertical resolution. This maximum setting provided a signal window of approximately 0.2 milliseconds at a frequency response of 10 megahertz. Because of the sequential storage of the digital signal in shift register memory, it was possible to retain the signal information preceding the trigger in time and therefore avoid loss of the leading edge of transients. This cannot be achieved easily with conventional oscilloscopes and is a very important feature when recording acoustic emission signals. Each recorded waveform was stored on a built-in minidisk magnetic memory for later analysis.

The signals stored in the magnetic disk memory by Bruchey (32) were transferred at a later time to a Hewlett-Packard 9845A computer for analysis. In more recent work the stored signals were transferred through interface of the Nicolet with a Tektronix 4006-1 Graphic Terminal to a DEC system-10 timesharing computer for analysis. The processed signal was also displayed on the Graphic Terminal and plotted on a 4662 Digital Plotter. Computer programs were written to produce graphic output of the captured signals and Fast Fourier Transform (FFT) frequency analysis of the time domain data. The option of analyzing either the whole waveform or only selected regions of interest was also available. Since the laser beam detector and the digital oscilloscope permitted the identification of signal frequencies as high as

10 megahertz and since this frequency is an order of magnitude higher than that recorded in previous acoustic emission studies, particular care was taken to be certain that any signal components received in the upper frequency realm were not an artifact of the optical probe, digital oscilloscope, or computer FFT analysis. Various calibrated test signals (sine waves and saw-tooth ramp functions) were fed into the system over the full frequency range. In all cases, the resultant FFT produced the expected frequency spectrum, centered on the signal frequency with very minimal off-frequency components. It was concluded that for the actual waveforms captured during the tensile loading experiments the waveform analysis truly indicates the frequencies present in the range 0-10 megahertz.

Micro-tensile specimens were tested in the pneumatic loading tensile machine until fracture. The rate of loading was adjusted such that specimen failure occurred within approximately 10-20 minutes; load versus time was recorded continuously until failure. In addition, a series of independent tensile tests was run using an Instron screw-drive tensile test machine. Because of the excessive background noise associated with this machine no acoustic emission measurements were attempted during these tests. Their purpose was to obtain engineering stress versus engineering strain curves for comparison with published engineering data to determine whether or not the small size of the micro-tensile specimens would cause anomalous behavior. Values obtained from standard engineering handbooks were in general agreement with this data, which demonstrated that although

the gauge section of the micro-tensile specimen was extremely small compared to that of standard engineering specimens, it was still large enough on a microstructural scale to assure that the acoustic emission signals recorded from the small gauge section were representative of the bulk material.

Before, during, and after each acoustic emission test, the surface of the gauge and sub-gauge section of each micro-tensile specimen was examined optically. Both optical and scanning electron microscope (SEM) examination showed that the surface did not contain any features which would confuse subsequent surface morphological alteration correlation with acoustic emission events. During tensile elongation the surface of the sub-gauge section lost its polish and appeared frosted. For this reason the optical probe was focused on a spot on the gauge section immediately adjacent to the deforming sub-gauge region. As tensile elongation proceeded, extensive formation of slip bands was observed in the austenite grains. Rotation of the individual grains resulting in considerable surface roughness was also observed. Prior to fracture, each specimen exhibited necking at the middle of the sub-gauge section, followed by a "Swiss cheese" appearance due to void nucleation and growth, and final failure by void coalescence and fracture of the remaining ligaments. Examination of specimens removed from the test fixture prior to fracture as well as those pulled to fracture failed to reveal any surface cracks. Fracture was definitely due to void coalescence.

Examination of the fracture surface of each failed specimen in the SEM at a magnification of 500X or greater revealed that each void contained a rather large intermetallic particle. At the base of some of these voids were particles that had cracked in a brittle manner. By scanning the entire fracture surface of the sub-gauge section and counting the number of cracked intermetallic particles, Bruchey found a near one-to-one correspondence between fractured intermetallic particle count and the number of acoustic emission bursts in the 7.5-8.5 megahertz regime. Although fracture of intermetallics have been offered by a number of authors in a number of materials as the source of emissions, this is believed to be the first time that direct counts, rather than statistical counts accompanied by unsubstantiated assumptions, support this hypothesis. It should be noted that the small sub-gauge size and flat frequency response of the optical probe up to at least 10 megahertz were both necessary for successful completion of such measurements.

Following completion of the 304L stainless steel tests several modifications were incorporated in the experimental measurement system to permit easier positioning of the laser beam and to increase the system stability. Since the magnetic diskette recorder incorporated with the Nicolet digital oscilloscope uses 8-channel diskettes, which have to be manually changed, a continuous record of all of the acoustic emission signals generated during a test were made using a Sony Model 3650 videotape recorder. Although, as described previously, the quality

of the signal is degraded somewhat by the video tape recorder, it does insure that no signals are missed completely and provides an accurate time record as to when selected signals are captured on the Nicolet.

Materials presently available for testing are 6Al 4V and 6Al 2Cb 1Ta 1Mo titanium alloys; HY80, HY100 and HY 130 steel; 2024, 5456, and 7039 aluminum alloys; pure zinc; and plexiglass. Primary effort is currently directed at the titanium and steel materials because they represent extremely important naval alloys. Some of the other materials are on hand mainly for comparison purposes.

At room temperature pure titanium possesses a hexagonal close-packed structure called alpha. At 1621°F(883°C) it transforms to a body-centered-cubic structure called beta. The addition of alloying elements modify this transformation temperature. Elements that favor the alpha phase, known as alpha stabilizers, raise the alpha to beta transformation temperature. Among the alpha stabilizers are aluminum, gallium, germanium, carbon, oxygen, and nitrogen. On the other hand, there are two groups of elements that favor the beta phase. These beta stabilizers, which lower the beta to alpha transformation temperature, includes vanadium. Vanadium also serves as a strengthening agent. Metallographic examination of the 6Al 4V titanium alloy revealed that there are approximately equal amounts of three types of alpha titanium present, namely martensitic, acicular, and platelike. Some alpha also appears at prior beta grain

boundaries. In addition to the alpha microstructures intergranular beta is observable.

Among the surface alterations caused by tensile elongation of the titanium specimens, observed by either optical or scanning electron microscopy, and which are possible sources of acoustic emission are slip bands, mechanical twins, microcracks, void creation and coalescence, and cavity formation. The microcracks and cavities were too few in number, while void coalescence occurred too late in the deformation process, to account for the primary acoustic emission observed.

Optical and scanning electron microscopic examination of the surface of the HY 80 specimens subsequent to tensile elongation revealed both slip bands and intermetallic particles. For this material the primary acoustic emissions were localized to a particular region of the loading curve.

Since the laser furnished by the Navy, which was to be used for double pulse laser holography, did not operate and since there were no funds available to purchase a new multi-thousand dollar laser, this particular part of the research was not conducted. Instead, a second laser detecting system, which incorporated a Michelson interferometer, was used to measure the propagational characteristics of simulated acoustic emission signals on specimens of several geometries. Measurements were initially performed on a 4-inch diameter steel sphere subjected to a step-function unloading force caused by breaking a glass capillary. This particular geometry was selected because prior

theoretical work in the field of seismology permitted Weisinger(34) to compute the surface displacement as a function of time for a step-function load applied to the surface of such a sphere. Preliminary experimental measurements appeared promising but ran into trouble because of the difficulty of reproducibly breaking a cylindrical glass capillary at any desired point on the spherical surface. The fact that this was indeed the problem was confirmed by repeating earlier measurements in which the glass capillaries were broken at the center of the flat face of a right circular cylinder.

It was also discovered that the laser beam detector being used for this portion of the experimental research was not sufficiently stable to be optimally used for the acoustic emission wave propagation characterization measurements. Fortunately, a superior laser beam interferometric surface displacement measurement system had been developed at the Johns Hopkins University Applied Physics Laboratory(APL), which exhibited excellent stability though limited to a maximum frequency of 6 kilohertz(37). Preliminary modifications (at APL expense) have indicate that the frequency response can be extended to at least 30 megahertz and that additional modifications will result in an ideal detector for the propagation characterization measurements.

REFERENCES

1. P. H. Hutton and R. N. Ord, "Acoustic Emission," in Research Techniques in Nondestructive Testing, Vol. 1, pp. 1-30, R. S. Sharpe, ed., Academic Press, London and New York (1970).
2. Acoustic Emission, R. G. Liptai, D. O. Harris, and C. A. Tattro, eds., ASTM STP 505, American Society for Testing and Materials, Philadelphia, Pa. (1972).
3. A. A. Pollock, "Acoustic emission, A review of recent progress and technical aspects," in Acoustics and Vibration Progress, Vol. 1, pp. 53-84, R. W. B. Stephens and H. G. Leventhal, eds., Chapman and Hall, London (1974).
4. J. C. Spanner, Acoustic Emission, Techniques and Applications, Intex Publishing Co., Evanston, Illinois (1974).
5. A. E. Lord, Jr., "Acoustic Emission," in Physical Acoustics, Vol. 11, pp. 289-353, W. P. Mason and R. N. Thurston, eds., Academic Press, New York (1975).
6. Monitoring Structural Integrity by Acoustic Emission, J. C. Spanner and J. W. McElroy, eds., ASTM STP 571, American Society for Testing and Materials, Philadelphia, Pa. (1975).
7. Acoustic Emission, R. W. Nichols, ed., Applied Science Publishers Ltd., London (1976).
8. Proceedings First Conference on Acoustic Emission/Microseismic Activity in Geologic Structures and Materials, H. R. Hardy, Jr., and F. W. Leighton, eds., Trans. Tech Publications, Clausthal, Germany (1977).
9. T. F. Droillard, Acoustic Emission, a Bibliography with Abstracts, F. J. Laner, ed., IFI/Plenum, New York (1979).
10. H. Dunegan and D. Harris, "Acoustic Emission - A New Nondestructive Testing Tool," Ultrasonics 7, 160-166 (1969).
11. P. Jax and J. Eisenblatter, "Acoustic Emission Measurements During Plastic Deformation of Metals," Information 15 Battelle Frankfurt, pp. 2-8 (April 1973).

12. F. R. Breckenridge, C. E. Tschiegg, and M. Greenspan, "Acoustic emission: some applications of Lamb's problem," *J. Acoust. Soc. Amer.* 57, 625-631 (1975).
13. N. N. Hsu, J. A. Simmons, and S. C. Hardy, "An Approach to Acoustic Emission Signal Analysis- Theory and Experiment," *Materials Evaluation* 35, 100-106 (1977).
14. N. N. Hsu and S. C. Hardy, "Experiments in Acoustic Emission Waveform Analysis for Characterization of AE Sources, Sensors and Structures," in Elastic Waves and Non-Destructive Testing of Materials, Y. H. Pao, ed., AMD - Vol. 29, pp. 85-106, The American Society of Mechanical Engineers, New York (1978).
15. C. H. Palmer and R. E. Green, Jr., "Optical Probing of Acoustic Emission Waves," in Nondestructive Evaluation of Materials, J. J. Burke and V. Weiss, eds., Sagamore Army Materials Research Conference, Raquette Lake, New York (1976), Conference Proceedings 23, 347-378, Plenum Press, New York, (1979).
16. R. E. Green, Jr., and C. H. Palmer, "Optical Detection of Acoustic Emission Waves," *Proceedings of the Ninth International Congress on Acoustics*, Madrid, Spain (July 1977).
17. C. H. Palmer and R. E. Green, Jr., "Optical Detection of Acoustic Emission Waves," *Applied Optics* 16, 2333-2334 (1977).
18. C. H. Palmer and R. E. Green, Jr., "Materials Evaluation by Optical Detection of Acoustic Emission Signals," *Materials Evaluation - Research Supplement* 35, 107-112 (1977).
19. C. H. Palmer and R. E. Green, Jr., "Optical Detection of Acoustic Emission Signals," *Proceedings of ARPA/AFML Review of Progress in Quantitative NDE Meeting*, Cornell University, Ithaca, New York (June 1977), AFML-TR-78-55 (may 1978).
20. C. H. Palmer, "Optical Detection of Ultrasonic Transients," *Proceedings of 1978 Conference on Information Sciences and Systems*, The Johns Hopkins University, Baltimore, Maryland, pp. 559-563 (1978).

21. R. A. Kline, "Optical and Piezoelectric Detection of Acoustic Emission Signals," Ph.D. Thesis, Mechanics and Materials Science Department, The Johns Hopkins University, Baltimore, Maryland (1978).
22. R. A. Kline, R. E. Green, Jr., and C. H. Palmer, "A Comparison of Optically and Piezoelectrically Sensed Acoustic Emission Signals," J. Acoust. Soc. Am. 64, 1633-1639 (1978).
23. C. H. Palmer, "Optical Measurement of Acoustic Emission at High and Low Temperatures," Proceedings of ARPA/AFML Review of Progress in Quantitative NDE Meeting, La Jolla, California (July 1978), AFML-TR-78-205 (January 1979).
24. C. H. Palmer and S. E. Fick, "New Optical Instrument for Acoustic Emission," IEEE Southeastcon, Roanoke, Virginia, pp. 191-192, (April 1979).
25. R. E. Green, Jr., B. B. Djordjevic, C. H. Palmer, and S. E. Fick, "Laser Beam Detection of Ultrasonic and Acoustic Emission Signals for Nondestructive Testing of Materials," Proceedings of ASM Conference on Applications of Lasers to Materials Processing, pp.161-175, Washington, D.C. (April 1979), American Society for Metals, Metals Park, Ohio (1979).
26. B. B. Djordjevic and R. E. Green, Jr., "High Speed Digital Capture of Acoustic Emission and Ultrasonic Transients as Detected with Optical Laser Beam Probes," Proceedings of Ultrasonics International 79 Conference, Graz, Austria (May 1979), pp. 82-87, IPC Science and Technology Press Ltd., Guildford, England (1979).
27. C. H. Palmer and R. E. Green, Jr., "Optical Probing of Acoustic Emission Waves," Final Report, U. S. Army Research Office, The Johns Hopkins University (August 1979).
28. B. B. Djordjevic, "Digital Waveform Recording and Computer Analysis of Acoustic Emission and Ultrasonic Transients Detected by Optical and Piezoelectric Probes," Ph.D. Thesis, Mechanics and Materials Science Department, The Johns Hopkins University, Baltimore, Maryland (1979).
29. R. E. Green, Jr., "Acoustic Emission," Encyclopedia of Science and Technology, McGraw-Hill, New York (to be published 1980).

30. R. A. Kline, R. E. Green, Jr., and C. H. Palmer, "Acoustic Emission Waveforms from Stress-Corrosion Cracking of Steel: Experiment and Theory (accepted for publication in J. Appl. Phys.).
31. A. Peterlin, B. B. Djordjevic, J. C. Murphy, and R. E. Green, Jr., "Acoustic Emission During Craze Formation in Polymers (submitted for publication in J. Appl. Phys.).
32. W. J. Bruchey, Jr., "Optical Probing of Acoustic Emission During Deformation of Micro-Tensile Specimens," Ph.D. Thesis, Materials Science and Engineering Department The Johns Hopkins University, Baltimore, Maryland (1980).
33. L. J. Graham and G. A. Alers, "Spectrum Analysis of Acoustic Emission in A-533-B Steel," Materials Evaluation 32, 31-37 (1974).
34. R. Weisinger, "Acoustic Emission and Lamb's Problem on a Homogeneous Sphere," Masters Essay, Mechanics and Materials Science Department, The Johns Hopkins University, Baltimore, Maryland (1979).
35. R. Weisinger, "Determination of Fundamental Acoustic Emission Signal Characteristics," Proceedings of Conference on Mechanics of Nondestructive Testing, W. W. Stinchcomb (ed.), Plenum Press, New York (1980), pp. 165-185.
36. R. E. Green, Jr., "Basic Wave Analysis of Acoustic Emission," Proceedings of Conference on Mechanics of Nondestructive Testing, W. W. Stinchcomb (ed.), Plenum Press, New York (1980), pp. 55-76.
37. A. N. Jette, M. S. Morris, J. C. Murphy, and J. G. Parker, "Active Acoustic Detection of Leaks in Underground Natural Gas Distribution Lines," Materials Evaluation Vol. 35, No. 10, pp. 90-99 (1977).

INITIAL DISTRIBUTION

Copies	CENTER DISRIBUTION	
	Copies	Code
1 ONR Code 471		
1 ONR Code 474		
4 NRL	1	17
1 Code 6307		
1 Code 6311		
1 Code 6380		
1 Code 6385		
2 Naval Air Development Center		
Naval Materials Center		
Warminster, PA 18974	1	2724
Code 6403		
Code 6063	1	280
12 NAVSEA	1	2803
1 SEA 03C		
1 SEA 03R	1	2809H
1 SEA 05E		
1 SEA 05R15	1	281
1 SEA 323		
1 SEA 3232	1	2812
1 SEA 90		
1 SEA 92	1	2813
2 SEA 996		
2 SEA 96612	1	2814
4 Naval Air Systems Command	1	282
Washington, DC 20361		
AIR - 320B	2	2820
AIR - 5163		
AIR - 5302	1	2821
AIR - 950D		
	1	2822
1 Chief of Naval Material		
Washington, DC 20360	1	2823
MAT0715		
	1	522.1
1 Naval Surface Weapons Center		
White Oak, MD 20910	2	5231
Attn: Mr. J. Agul		
50 The Johns Hopkins University		
Materials Science and Engineering Department		
Baltimore, MD 21218		
Attn: Dr. R. E. Green, Jr.		
12 DTIC		

INITIAL DISTRIBUTION

AFWAL

Wright Patterson AF Base, Ohio 45433
 Attn: Mr. P. A. Parmley

Air Force Office of Scientific Research
 Bldg 410, Bolling AFB
 Washington, DC 20332
 Attn: Mr. LT COL J. Morgan

NASA

Langley Research Center
 Hampton, VA 23365
 Attn: Dr. J. Davidson

Army Air Mobility R&D Laboratory
 Fort Eustis, VA 23604
 Attn: SAVDL-EU-SS (Mr. J. Robinson)

Army Material & Mechanics Research Center
 Watertown, Mass 02172
 Attn: Dr. E. Lenore

Army Mobility R&D Laboratory
 Ames Research Center
 Moffett Field, CA 94035
 Attn: Dr. Raymond Foye

Army Research Office
 Research Triangle Park, NC 27709
 Attn: Dr. F. Schmiedeshoff

Boeing Vertol Company
 Philadelphia, PA 19142
 Attn: Mr. E. C. Durchlaub

McDonnell Douglas Corporation
 Douglas Aircraft Co.
 3855 Lakewood Blvd.
 Long Beach, CA 90801
 Attn: Mr. L. Gresczuk

Northrop Corporation
 3901 West Broadway
 Hawthorne, CA 90250
 Attn: Dr. N. Bhatia

General Dynamics
 Convair Aerospace Division
 Fort Worth, TX 76101
 Attn: Dr. R. Wilkins

Lockheed-California Co.
 Burbank, CA 91503
 Attn: Mr. F. English

Vought Corporation
 Advanced Technology Center
 Dallas, TX 75266
 Attn: Dr. J. Renton

Grumman Aerospace Corporation
 Bethpage, NY 11714
 Attn: Mr. R. Hadcock

Sikorsky Aircraft
 Stratford, CO 06602
 Attn: Mr. M. J. Rich

Boeing Aircraft Corporation
 P.O. Box 3707
 Seattle, Washington 98124
 Attn: Mr. E. House

Lear Fan Corporation
 Reno Nevada 89506
 Attn: Mr. R. Abbott

Hughes Helicopter
 Culver City, CA 90230
 Attn: Mr. R. Moore

Rockwell International
 Downey, CA 90241
 Attn: Mr. W. H. Morita

Bell Helicopter Textron
 Fort Worth, TX 76101
 Attn: Mr. R. Alsmiller

Kaman Aerospace Corporation
 Bloomfield, CO 06002
 Attn: Mr. L. Schuler

Lockheed Missiles & Space Co.
 Sunnyvale, CA 94088
 Attn: Mr. H. Marshall